Nuclear Engineering and Technology 53 (2021) 793–803

Contents lists available at ScienceDirect

Nuclear Engineering and Technology

journal homepage: www.elsevier.com/locate/net

Original Article

Scaling analysis of the pressure suppression containment test facility for the small pressurized water reactor

Xinxing Liu, Xiangjie Qi, Nan Zhang, Zhaoming Meng*, Zhongning Sun

Fundamental Science on Nuclear Safety and Simulation Technology Laboratory, Harbin Engineering University, Harbin, Heilongjiang 150001, China

ARTICLE INFO

Article history:
Received 30 June 2020
Received in revised form
8 August 2020
Accepted 28 August 2020
Available online 10 September 2020

Keywords:
Scaling analysis
Small PWR
Top-down
Bottom-up
H2TS

ABSTRACT

The small PWR has been paid more and more attention due to its diversity of application and flexibility in the site selection. However, the large core power density, the small containment space and the rapid accident progress characteristics make it difficult to control the containment pressure like the traditional PWR during the LOCA. The pressure suppression system has been used by the BWR since the early design, which is a suitable technique that can be applied to the small PWR. Since the configuration and operating conditions are different from the BWR, the pressure suppression system should be redesigned for the small PWR. Conducting the experiments on the scale down test facility is a good choice to reproduce the prototypical phenomena in the test facility, which is both economical and reasonable. A systematic scaling method referring to the H2TS method was proposed to determine the geometrical and thermohydraulic parameters of the pressure suppression containment response test facility for the small PWR conceptual design. The containment and the pressure suppression system related thermohydraulic phenomena were analyzed with top-down and bottom-up scaling methods. A set of the scaling criteria were obtained, through which the main parameters of the test facility can be determined.

1. Introduction

With the large-scale application of the nuclear energy, the nuclear safety has attracted more and more attention, especially after the Fukushima nuclear power plant accident in Japan. As the last barrier to prevent the leakage of the radioactive materials, the containment is of great importance to the nuclear power plant, inside which the pressure and the temperature must be controlled below the allowable limit to ensure its integrity during the accident.

When the loss of coolant accident (LOCA) or the main steam line rupture accident (MSLB) occurs, a large amount of high-temperature and high-pressure water released from the reactor primary loop will flash evaporate, leading to the pressure rapidly rising in the containment. In order to deal with this kind of over-pressure problem, the large PWR nuclear power plants usually adopt the large volume containment design to slow down the pressure rise rate. Besides, the containment spray system (EAS) and the passive containment cooling system (PCS) are responsible for controlling the long-term pressure of the containment.

The small PWR has been paid more and more attention due to its diversity of application and flexibility in the site selection. Different from the traditional large PWR nuclear power plant, the small PWR generally has the characteristics of large core power density, small containment space, and rapid accident progress. Once the LOCA or the MSLB occurs, it is difficult to use the volume of the containment to quickly relieve the rising pressure. Besides, the EAS and the PCS are too late to play their role due to the limits of the start-up conditions and the response time. According to the numerical research of Quan et al. [1], the pressure came up to the peak value (0.75 MPa) after 40 s of a postulated design-basis LOCA accident without any pressure control measures in a 100 MWe reactor containment, which is beyond the design safety limit value.

Comparing to the traditional large PWR containment, the containment volume used in the BWR is very small. It is obvious that the small PWR and BWR both have the similar restrictions that the containment pressure should be controlled under the limit value in such a relatively small volume. In the BWR, the passive pressure suppression system is used to deal with the short-term overpressure problem of the containment after the accident. Once the pressure difference between the containment and the suppression pool exceed the blow down pipe hydrostatic head, the

* Corresponding author.
E-mail address: mengzhaoming@hrbeu.edu.cn (Z. Meng).

https://doi.org/10.1016/j.net.2020.08.024

steam and air mixture in the containment will be driven to the suppression pool. The process is totally passive and requires no external start signal. The large amount of steam will be condensed in the pool through direct contact condensation, which is highly efficient. The non-condensable gas will be contained in the suppression pool gas space after the water filtering process. It is a mature technique that has been adopted since the early BWR design. Comprehensively considering the existing post-accident containment pressure relief technology, the containment passive suppression technology is undoubtedly the best choice for the design of the small PWR pressure suppression systems.

Due to the complex thermal hydrodynamic phenomena of the suppression pool system, the containment pressure response is influenced by many factors. The experiments should be conducted to verify whether the pressure suppression containment can meet the demand for the small PWR containment peak pressure suppression in the early stage of the LOCA. Besides, the configuration and the operation condition between the BWR and the small PWR are different, it is inappropriate to directly apply the BWR pressure suppression system design to the small PWR. For this reason, the experiments should be specially designed for the small PWR to evaluate the pressure suppression system effect.

As for the BWR research, a lot of experimental investigation work in different scales on the pressure suppression containment have been carried out. The Marviken power plant in Sweden was originally designed and built as a boiling heavy water reactor [2,3]. Instead of being operated, the Marviken pressure suppression containment was used in performing full scale blow down experiments to study the containment response. JAERI had built a test facility to study the containment response during the LOCA [4], of which the lower portion of the test containment is a full-scale replica of one of the 20° sectors in the annular wetwell of a typical MARK II containment. The test facility features seven full size vent pipes. The drywell and the primary system are represented in the same volumetric scale ratio (1:18) as the wetwell. LUT in Finland had conducted a series of experiments in PPOOLEX program to investigate the suppression pool related thermal hydraulic phenomena [5–7]. The PPOOLEX test facility is a scaled down test facility of Nordic type BWR containment. The 31 m^3 stainless steel containment consists of two main parts, i.e. the drywell compartment and the wetwell compartment, separated by an intermediate floor. The volume of the two parts and the diameter of the blow down pipe were just linearly scaled according to the Olkiluoto nuclear power plant prototype parameters, while more scaling parameters was not given in their reports.

Although the full-scale experiment can predict the real pressure evolution with the most limited deviation, such experiments are both costly and hard to operate. Therefore, the most acceptable methods of predicting the pressure response in the containment are through the scale models and simulation experiments, using the scaling laws to extrapolate the simulation results to full scale prototype transients. However, it is necessary that the scaling rationale be logical and reasonable. Scaling laws and scaling criteria thus become the most important issue for designing, performing, and analyzing simulation experiments using a scale model. Unfortunately, there are no systematic and specific scaling methods for the experimental work mentioned above in the public literature. Beyond that, the scaling analysis aiming at the pressure suppression system is also rare. Therefore, it is necessary to analyze the thermohydraulic phenomena in the pressure suppression system of the small PWR and propose the scaling methods suitable for the test facility design.

In this paper, a systematic scaling method referring to the H2TS method was proposed to determine the geometrical and thermal hydraulic parameters of the pressure suppression containment response test facility for the small PWR conceptual design. The general scaling method was introduced firstly, therewith the dominant phenomena identification, and then the top-down scaling analysis focused on the systematic response and the bottom-up scaling analysis focused on the local phenomena. At last, the dimensionless similarity criteria were developed to determine the geometrical dimensions and experimental conditions of the test facility.

2. Scaling methods

The scaling analysis is a method developed to establish a scale-down experimental facility that can simulate the process of the prototype accidents. Its essence is to simplify the reference prototype into an experimental model by reducing the geometric size and changing the fluid properties according to the similarity theory but still ensure that the phenomena concerned is reproduced well in the experiment.

There are various scaling methods according to different scaling logic. The linear scaling is a kind of simple method, in which all the linear dimensions are reduced by the same proportion. Although it is suitable for some single-phase flow situations, the linear scaling also brings about the thermal and flow distribution distortions when it comes to the two-phase flow conditions, [8,9]. Besides, the acceleration scale has to be reduced by $1/L_R$, which is difficult to satisfy for the vertical gravity acceleration. For these reasons, the power/volume scaling is developed based on the linear scaling. The velocity ratio, the time ratio, the length ratio and the power ratio in the power/volume scaling is equal to 1, therefore, the test data can be used directly to analyze and predict the important transients in the prototype. The weakness of the power/volume scaling is that the scaled test facility is usually tall and thin, which results in a remarkable increased resistance due to the reduced cross-sectional area. In addition, the rather large surface area/volume ratio leads to the system heat loss larger than the scaled value, resulting in distortion of the slow transients. Both linear and power/volume scaling methods described above are developed based on single-phase flow conservation equations. However, extending these methods to investigate phenomena associated with two-phase flow, particularly for non-homogeneous flows, is certainly incorrect. Zuber et al. [10] proposed the hierarchical two-tiered scaling (H2TS) method, which is a structured scaling analysis method for analyzing the complex multiphase flow systems. The conduction of the H2TS method mainly consists of four parts: the system decomposition, the scale identification, the top-down scaling analysis and the bottom-up scaling analysis. It can ensure both the similarity of the whole system and the similarity of the local important phenomena. The top-down approach provides non-dimensional scaling groups (Π-groups) in terms of time ratios that characterize system response to a given transfer process, while the bottom-up approach focuses on the important processes to maintain applicability of the data by addressing order of progression and process bifurcations. And it provides the closure relations for the characteristic time ratios given by the top-down scaling analysis. H2TS is an advanced method that is suitable for integral facility scaling. It has been successfully applied to a series of scale-down modeling of nuclear safety related experiments [11,12], especially the experiments related to the containment.

The main purpose of the construction of the scale down test facility is to verify whether the pressure suppression capability of the designed containment passive pressure suppression system meets the demand of the prototype small PWR. The containment pressure response characteristic is the most important physical phenomena that the scale down experiment needs to reproduce. Therefore, the dominant phenomena occurred in the related

system should be identified at first, and then the top-down modeling analysis of the pressure response characteristics of the containment and suppression system should be performed at the system level to obtain the corresponding characteristic time ratio and the similarity criterion. Built on this, the bottom-up modeling analysis of important local physical parameters of the containment and suppression system is also needed to obtain similarity criteria to ensure that these physical processes are reproduced in the experiment. Hence, for the design of the experimental facility of the passive containment pressure suppression system, it is planned to carry out the scaling analysis by means of the H2TS method. The procedure of the scaling analysis conducting is shown in Fig. 1.

3. Scaling analysis

3.1. Dominant phenomena identification

The exact similitude between the test facility and the prototype is not allowed due to the nature of the scaling, thus the dominant and most important phenomena should be picked out among all related thermohydraulic phenomena and analyzed with the scaling methods. Sawant et al. [13] came up with the phenomena identification ranking table (PIRT) applicable to advanced boiling water reactor (ABWR) containment pressure-temperature and suppression pool swell response during the design basis accidents, which is a suitable reference to the dominant phenomena identification in this paper.

From the systematic aspect, containment pressure response is the most concerned phenomenon, which is determined by the mass and energy release, transfer and transportation process in the containment. Therefore, the reactor primary loop coolant inventory is of great importance, which should also be scaled to match the mass and energy released to the containment. Meanwhile, as the steam and non-condensable gas heat and mass sink, the pressure suppression system plays a role in the system pressure response as well. All these three terms will be properly scaled to provide the initial form of the similarity criteria.

From the local phenomena aspect, various individual processes contribute to the overall response respectively:

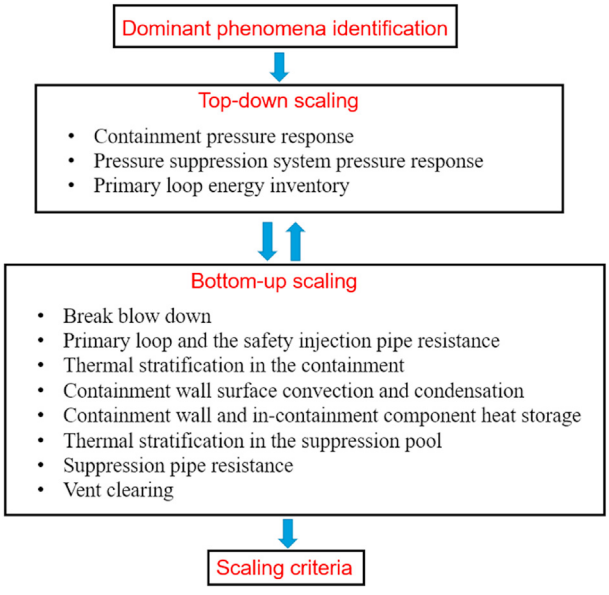

Fig. 1. Scaling analysis flow chart.

(1) Break blow down process. During the accident, the primary loop coolant blow down from the break is the main mass and energy source entering into the containment. The fluid flow state (such as the fluid velocity) at the break will influence the mass and energy transport rate, which has an effect on the containment pressure rise rate. Thus, the fluid flow state at the break is a key parameter needs to be preserved.

(2) Reactor primary loop resistance and the safety injection pipe resistance. When the break accident occurs, the resistance characteristics of the primary loop directly affects the pressure of the fluid at the break, which in turn affects the flow state of the fluid, and indirectly affects the thermohydraulic state in the containment after the accident. The resistance characteristics of the safety injection system directly affects the safety injection flow rate and has an impact on the accident process.

(3) Thermal stratification in the containment. The discharge of a large amount of steam after the accident will affect the temperature in the containment and the stratification of the non-condensable gases. The temperature in the containment and the stratification of the non-condensable gas will affect the dynamic response characteristics and the suppression capability of the suppression system. Therefore, it is necessary to model the thermal stratification in the containment so that the thermal stratification phenomena can be preserved in the experiment.

(4) Containment wall surface convection and condensation. During the accident, the mixed hot gas flows in the containment space and contacts with the cold containment wall, thus the heat transfer and steam condensation occurs. These processes act as the mass and energy sink, contributing to the containment depressurization.

(5) Containment wall and in-containment component heat storage. There are a variety of metal structures and non-metal structures in the prototype containment. In the break accident, these structures will act as the short-term heat sinks (e.g., metal) or the long-term heat sinks (e.g., concrete) to directly absorb the energy in the containment, which in turn affects the thermal hydraulic conditions in the containment after the accident.

(6) Thermal stratification in the suppression pool. Thermal stratification and mixing phenomena have been investigated by many researchers [14,15]. Based on the research of Gamble et al. [16], the long-term post-accident containment pressure is determined by the combination of non-condensable gas pressure and steam pressure in the wet well gas space. The suppression pool surface temperature, which determines the vapor partial pressure, is especially important to overall containment performance. According to the heat balance, when the total volume of the water in the suppression pool is known, the homogenous temperature increase of the water can be calculated. However, if the thermal stratification appears in the water space, the actual pool surface temperature will be higher than the calculated value. In the Fukushima accident, Unit 3 had a rapid pressure rise in the containment in the early accident due to the thermal stratification in the water space of the suppression pool, which resulted in the reduction of the suppression capability of the suppression system [17]. Therefore, it is necessary to model the thermal stratification phenomena in the suppression pool, so that the similar thermal stratification to the prototype can be preserved in the experiment.

(7) Suppression pipe resistance. The suppression pipe is a key component connecting the containment and the suppression pool. Higher pressure drop of the suppression pipe leads to

higher containment pressure and lower vent flow rate. Therefore, in order to ensure that the pressure response of the containment and the suppression system is similar after the accident, the pressure drop of the suppression pipe in the prototype and the experiment should be equal.

(8) Vent clearing process. The suppression pipe is immersed in the pressure suppression pool. When the accident occurred, the water column in the suppression pipe must be completely extruded before the steam start to discharge, which means the direct contact condensation with the sub-cooled water in the suppression pool can occur only after the vent clearing phase stops. Based on boiling water reactor research experience, the vent clearing phase time is usually between 0.8 and 2s. The length of the vent clearing phase time is related to the pressure response characteristics of the containment after the accident. Therefore, it is necessary to model the vent clearing process in the experiment.

The specific processes considered above provide the closure relations for the initial form systematic scaling criteria to be completed to the final form ones.

3.2. Assumptions

In order to make the derivation of the scaling analysis clear and easy to conduct, some reasonable and conservative assumptions are presented below:

(1) The gas volume of the containment is assumed to be constant, which means dV/dt ≈ 0. Although the liquid coolant and the condensate water will be released to the containment, the total amount of the liquid is negligible comparing to the containment volume.
(2) The containment atmosphere is considered as an air-steam, ideal gas mixture.
(3) The same working fluid is used with the prototypical thermodynamic conditions in the test facility, which both simplifies the scaling ratios and avoids some scaling of the internal energy partial derivates terms.
(4) The primary energy transfer mechanisms in the containment consist of condensation, convection and the energy transportation to the pressure suppression system. The outside wall of the containment is assumed to be adiabatic only in the early stage due to the fast transient, while the heat convection between the outside wall and the environment atmosphere should be considered in the long-term accident.
(5) The temperature gradient of the containment wall is assumed to be 0, which means the containment wall outside and inside temperature is equal.
(6) The radiation heat exchange of the in-containment structures and the containment wall is neglected.

3.3. Top-down scaling analysis

3.3.1. Containment pressure response scaling

Taking the free volume inside the containment as the control body, as shown in Fig. 2, there are four primary items that affect the containment pressure, which are the break blow down energy, the steam condensation, the heat convection through the solid surface (the containment wall and the in-containment heat structure), and the energy transported to the suppression pool. Therefore, the rate of pressure change (RPC) equation of the containment control volume is derived as:

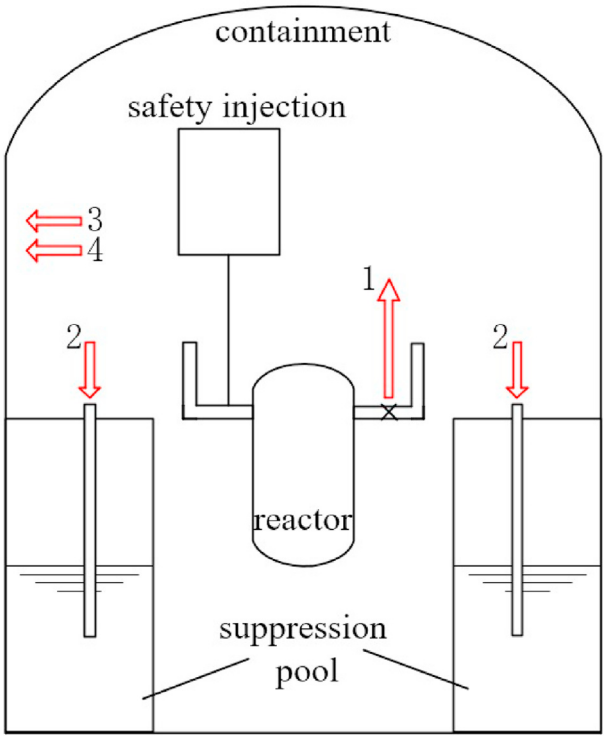

Fig. 2. Schematic diagram of the conceptual small PWR: (1) break blow down energy; (2) energy transported to the suppression pool; (3) condensation heat transfer; (4) convection heat transfer inside the containment.

$$\frac{V}{\gamma-1}\frac{dp}{dt}=\dot{m}_{brk}i_{brk}-\dot{m}_{in}i_{stm}-\dot{m}''_{cond}A_{cond}i_{stm}-h_{conv}A_{conv}\left(T_s-T_{srf}\right) \quad (1)$$

By normalizing with appropriate reference values (i.e. $X^+ = X/X_{ref}$, see in Table 1), the variables in the above dimensional form of the RPC equation can be put into non-dimensional form as:

$$\frac{V^+}{\gamma-1}\frac{dp^+}{dt^+}=\left\{\frac{\dot{m}_{brk,0}i_{brk,0}}{V_0p_0}\tau_{cv}\right\}\dot{m}^+_{brk}i^+_{brk}-\left\{\frac{\dot{m}_{in,0}i_{stm,0}}{V_0p_0}\tau_{cv}\right\}\dot{m}^+_{in}i^+_{stm}-\left\{\frac{\dot{m}''_{cond,0}A_{cond,0}i_{stm,0}}{V_0P_0}\tau_{cv}\right\}\dot{m}''^+_{cond}A^+_{cond}i^+_{stm}-\left\{\frac{h_{conv,0}A_{conv,0}\left(T-T_{srf}\right)_0}{V_0p_0}\tau_{cv}\right\}h^+_{conv}A^+_{conv}\Delta T^+_{srf} \quad (2)$$

The four coefficient terms on Eq. (2) right-hand side represent the characteristic time ratios, which characterize the time ratio of the system response time τ_{cv} to the specific transfer process time. In this way, all transfer processes can be evaluated in terms of the system response time only [10]. To make the prototype containment pressure response process resemble the experimental pressure response process, these four characteristic time ratios of the test facility to the prototype must equal to 1:

$$\prod_{p,Co,brk,R}=\left\{\frac{\dot{m}_{brk,0}i_{brk,0}}{V_0p_0}\tau_{cv}\right\}_R=1 \quad (3)$$

Table 1
RPC equation variables nondimensionalization.

Parameters	Nondimensionalized variables
Containment free volume	$V^+ = \frac{V}{V_0}$
Containment pressure	$p^+ = \frac{p}{p_0}$
Time	$t^+ = \frac{t}{\tau_{cv}} = \frac{t}{V_0 \Big/ \dot{Q}_{brk,0}}$
Break steam mass flow rate	$\dot{m}^+_{brk} = \frac{\dot{m}_{brk}}{\dot{m}_{brk,0}}$
Break steam enthalpy	$i^+_{brk} = \frac{i_{brk}}{i_{brk,0}}$
Seam mass flow rate transported to the pressure suppression system	$\dot{m}^+_{in} = \frac{\dot{m}_{in}}{\dot{m}_{in,0}}$
Solid surface steam condensation mass transfer flux	$m''^+_{cond} = \frac{\dot{m}''_{cond}}{\dot{m}''_{cond,0}}$
Solid surface steam condensation area	$A^+_{cond} = \frac{A_{cond}}{A_{cond,0}}$
Containment steam enthalpy	$i^+_{stm} = \frac{i_{stm}}{i_{stm,0}}$
Solid surface convection heat transfer coefficient	$h^+_{conv} = \frac{h_{conv}}{h_{conv,0}}$
Solid surface convection heat transfer area	$A^+_{conv} = \frac{A_{conv}}{A_{conv,0}}$
Temperature difference between the solid surface and the containment atmosphere	$\Delta T^+_{srf} = \frac{(T_s - T_{srf})}{(T_s - T_{srf})_0}$

$$\prod_{p,Co,in,R} = \left\{ \frac{\dot{m}_{in,0} i_{stm,0}}{V_0 p_0} \tau_{cv} \right\}_R = 1 \tag{4}$$

$$\prod_{p,Co,cond,R} = \left\{ \frac{\dot{m}''_{cond,0} A_{cond,0} i_{stm,0}}{V_0 p_0} \tau_{cv} \right\}_R = 1 \tag{5}$$

$$\prod_{p,Co,conv,R} = \left\{ \frac{h_{conv,0} A_{conv,0} \left(T - T_{srf}\right)_0}{V_0 p_0} \tau_{cv} \right\}_R = 1 \tag{6}$$

Because the same fluid (water vapor and air) are both used in the test facility and the prototype, and that the containment pressure response similarity between the prototype and the test facility is the aim of the scaling analysis, the thermal physical properties of the gas in the test facility remain the same as the prototype. In addition, since condensation and convection heat exchange occur on the same solid surface, the condensation area is equal to the convective area. When the characteristic time is preserved in the scaled down test facility, that is,

$$\tau_{cv,R} = 1 \tag{7}$$

Then, the above Eqs. (3)–(6) can be simplified as:

$$\prod_{p,Co,brk,R} = \left\{ \frac{\dot{m}_{brk,0} i_{brk,0}}{V_0} \right\}_R = 1 \tag{8}$$

$$\prod_{p,Co,in,R} = \left\{ \frac{\dot{m}_{in,0}}{V_0} \right\}_R = 1 \tag{9}$$

$$\prod_{p,Co,cond,R} = \left\{ \frac{\dot{m}''_{cond,0} A_w}{V_0} \right\}_R = 1 \tag{10}$$

$$\prod_{p,Co,conv,R} = \left\{ \frac{h_{conv,0} A_w}{V_0} \right\}_R = 1 \tag{11}$$

where A_w is the containment wall surface area, which is equal to the solid surface steam condensation area and the convection heat transfer area.

Based on Eqs. (8) and (9), the ratio of the break blow down energy and the steam mass flow rate from the containment to the suppression pool can be obtained when the scale ratio of the containment volume is determined. The ratio of the containment wall surface area will be discussed in the bottom-up scaling analysis when the related local phenomena are analyzed.

3.3.2. The pressure response in the suppression system scaling

According to the principle of the energy conservation, one part of the energy entering the suppression system is absorbed by the subcooled water in the suppression pool and the heat structures of the suppression system wall, another part is stored in the gas space. Then the relations of these energy can be expressed as Eq. (12),

$$\dot{m}_{in} i_{stm} = \dot{m}_{pool,l} c_{p,pool,l} \Delta T_{pool,l} + \dot{m}_{pool,g} i_{pool,g} + m_{stl} c_{p,stl} \Delta T_{stl} \tag{12}$$

Taking the atmosphere volume inside the suppression system as the control body, the main effect that influence the pressure of the suppression system is the energy entering the suppression system atmosphere volume. The rate of pressure change equation is derived as:

$$\frac{V_{pool,g}}{\gamma - 1} \frac{dp_{pool,g}}{dt} = \dot{m}_{pool,g} i_{pool,g} \tag{13}$$

Substitute Eq. (12), then

$$\frac{V_{pool,g}}{\gamma - 1} \frac{dp_{pool,g}}{dt} = \dot{m}_{in} i_{stm} - m_{pool,l} c_{p,pool,l} \Delta T_{pool,l} - m_{stl} c_{p,stl} \Delta T_{stl} \tag{14}$$

By normalizing with the same method in Table 1, the variables in the above dimensional form of the RPC equation can be put in non-dimensional form as:

$$\frac{V^+_{pool,g}}{\gamma-1}\frac{dp^+_{pool,g}}{dt}=\left\{\frac{\dot{m}_{in,0}i_{stm,0}}{V_{pool,g,0}p_{pool,g,0}}\tau_{cv}\right\}\dot{m}^+_{in}i^+_{stm}-\left\{\frac{m_{pool,l,0}c_{p,pool,}\Delta T_{pool,l,0}}{V_{pool,g,0}p_{pool,g,0}}\tau_{cv}\right\}m^+_{pool,l}c^+_{p,pool,l}\Delta T^+_{pool,l}-\left\{\frac{m_{stl,0}c_{p,stl,0}\Delta T_{stl,0}}{V_{pool,g,0}p_{pool,g,0}}\tau_{cv}\right\}m^+_{stl}c^+_{p,stl}\Delta T^+_{stl} \tag{15}$$

Since the same working fluid (steam, air and water) and material (stainless steel) as the prototype are used in the experimental facility, the thermal physical properties of the gas/liquid/stainless steel in the experiment and the prototype are the same. To resemble the suppression system pressure response of the experiment with the prototype, the following simplified dimensionless similarity criteria must be met:

$$\prod_{p,Sp,in,R}=\left\{\frac{\dot{m}_{in,0}}{V_{pool,g,0}}\right\}_R=1 \tag{16}$$

$$\prod_{p,Sp,pool,R}=\left\{\frac{m_{pool,l,0}\Delta T_{pool,l,0}}{V_{pool,g,0}}\right\}_R=1 \tag{17}$$

$$\prod_{p,Sp,stl,R}=\left\{\frac{m_{stl,0}\Delta T_{stl,0}}{V_{pool,g,0}}\right\}_R=1 \tag{18}$$

Substitute Eq. (9), Eq. 16–18 are simplified as:

$$\prod_{p,Sp,in,R}=\left\{\frac{V_0}{V_{pool,g,0}}\right\}_R=1 \tag{19}$$

$$\prod_{p,Sp,pool,R}=\left\{\frac{m_{pool,l,0}\Delta T_{pool,l,0}}{V_0}\right\}_R=1 \tag{20}$$

$$\prod_{p,Sp,stl,R}=\left\{\frac{m_{stl,0}\Delta T_{stl,0}}{V_0}\right\}_R=1 \tag{21}$$

According to Eq. 19–21, the scale ratio of the pressure suppression system gas volume, water volume and the mass of the heat structure in the test facility are determined.

3.3.3. Primary loop energy scaling

The break energy released to the containment mainly comes from the flash evaporation process of the high pressure, high temperature water in the primary loop. The process is influenced by the core decay heat and the safety injection water flow rate. The primary loop energy balance equation is expressed as:

$$\frac{d\left(m_{loop}i_{loop}\right)}{dt}=Q_{decay}+\dot{m}_{ecc}i_{ecc}-\dot{m}_{brk}i_{brk} \tag{22}$$

where on the equation left-hand side is the primary loop energy change rate, the first term on the equation right-hand side is the core decay heat power, the second term is the safety injection water energy flow, and the third term is the released break energy flow. By normalizing Eq. (22) with appropriate reference values, the energy balance equation can be generalized as:

$$\frac{d\left(m^+_{loop}i^+_{loop}\right)}{dt}=\left\{\frac{Q_{decay,0}}{m_{loop,0}i_{loop,0}}\tau_{cv}\right\}Q^+_{decay}+\left\{\frac{\dot{m}_{ecc,0}i_{ecc,0}}{m_{loop,0}i_{loop,0}}\tau_{cv}\right\}\dot{m}^+_{ecc}i^+_{ecc}-\left\{\frac{\dot{m}_{brk,0}i_{brk,0}}{m_{loop,0}i_{loop,0}}\tau_{cv}\right\}\dot{m}^+_{brk}i^+_{brk} \tag{23}$$

If the break energy release in the experiment resembles the prototype, the following non-dimensional similarity criteria must be met:

$$\prod_{p,Pr,brk,R}=\left\{\frac{\dot{m}_{brk,0}i_{brk,0}}{m_{loop,0}i_{loop,0}}\right\}_R=1 \tag{24}$$

$$\prod_{p,Pr,ecc,R}=\left\{\frac{\dot{m}_{ecc,0}i_{ecc,0}}{m_{loop,0}i_{loop,0}}\right\}_R=1 \tag{25}$$

$$\prod_{p,Pr,decay,R}=\left\{\frac{Q_{decay,0}}{m_{loop,0}i_{loop,0}}\right\}_R=1 \tag{26}$$

According to Eq. (8), the break energy release should be scaled based on the containment volume ratio, then equation (24) is simplified as:

$$\prod_{p,Pr,brk,R}=\left\{\frac{V_0}{m_{loop}i_{loop}}\right\}_R=1 \tag{27}$$

Similarly, Eq. (25)-(26) is simplified as:

$$\prod_{p,Pr,ecc,R}=\left\{\frac{\dot{m}_{ecc,0}i_{ecc,0}}{V_0}\right\}_R=1 \tag{28}$$

$$\prod_{p,Pr,decay,R}=\left\{\frac{Q_{decay,0}}{V_0}\right\}_R=1 \tag{29}$$

Based on Eq. 27–29, when the containment volume scale ratio is determined, the scale ratio of the primary loop water inventory, the core decay heat and the safety injection water flow rate can also be determined.

3.4. Bottom-up scaling analysis

3.4.1. Break blow down scaling

The fluid flow state at the break is a key parameter that determines the thermodynamic properties of the containment during an accident. According to different accidents and different stages of the blow down process, the blow down may be based on steam-water two phase discharge or saturated steam discharge.

In the early stage of the accident, the pressure in the reactor is much higher than the pressure in the containment, so the critical flow condition can be assumed. The critical mass flow is calculated as [18]:

$$\dot{m}_{brk}=G_cA_{brk} \tag{30}$$

For the saturated steam critical discharge, Eq. (31) can be obtained according to Moody's relation [19].

$$G_c=\left(\frac{2}{\gamma+1}\right)^{\frac{\gamma+1}{2(\gamma-1)}}\left(\gamma\rho_{g,0}p_0\right)^{1/2} \tag{31}$$

For the steam-water two phase discharge [20], Eq. (32) can be obtained.

$$G_c = \left[\left(v_{g,brk} - v_f \right) \frac{x_{brk}}{0.14 s_{fg,brk}} \left(\frac{ds_f}{dp} \right)_{brk} \right]^{-0.5} \tag{32}$$

Substitute Eq. (8), the similarity ratio of the critical discharge process is

$$\left(\frac{V_0}{G_c A_{brk} i_{brk,0}} \right)_R = 1 \tag{33}$$

In the middle and late stages of the accident, the break discharge process conforms to the hypothesis of the isentropic flow for short-pipe, and then the following energy balance equation can be obtained:

$$dh + d\frac{u^2}{2} = 0 \tag{34}$$

For the subcritical flow whose flow rate changes with the back pressure, Eq. (34) shows that under this condition, the conversion process from pressure potential energy to kinetic energy is considered, while the external heat transfer process of the flow is ignored. Therefore, the flow equation in the tube can be obtained as:

$$\frac{d(\rho u \delta)}{dt} = \Delta\left(\rho u^2\right) + \Delta p - \frac{\rho u^2 \left(K_{srk} + K_{\exp}\right)}{2} \tag{35}$$

Ignoring the effect of the fluid flow velocity in the break, and taking the break form loss coefficient as $K_{srk} + K_{exp} = 0.5$, Eq. (35) is simplified as:

$$\frac{3\rho u^2}{4} - \frac{\rho u \delta}{t} + \Delta p = 0 \tag{36}$$

where t is the time required for the fluid to pass through the thickness of the break.

Ignoring the effect of fluid flow velocity and assuming the break flow is a uniformly accelerated motion that starts from rest, and then the relationship between the motion time, the fluid acceleration and the break thickness is shown as follow:

$$u^2 = 2a\delta \tag{37}$$

$$\delta = \frac{at^2}{2} \tag{38}$$

Combine Eqs. (36)–(38), then

$$\frac{\rho u^2}{4} + \Delta p = 0 \tag{39}$$

The break flow velocity and the flow rate can be calculated as:

$$u = 2\sqrt{\frac{|\Delta p|}{\rho}} \tag{40}$$

$$G_{non-c} = 2\sqrt{|\Delta p| \rho} \tag{41}$$

Substitute Eq. (8), the similarity condition for subcritical discharge is

$$\left(\frac{V_0}{G_{non-c} A_{brk} i_{brk,0}} \right)_R = 1 \tag{42}$$

Based on Eq. (33) and Eq. (42), the break area scale ratio can be determined.

3.4.2. Primary loop resistance and the safety injection pipe resistance scaling

To keep the resistance characteristics of the prototype and the experiment to be similar, the equation below should be met,

$$\left\{ \left(\frac{f_i l_i}{d_i} + \sum_i K_i \right) \frac{\dot{m}_i^2}{2\rho A_i^2} \right\}_R = 1 \tag{43}$$

where, f and K represent the resistance coefficient and the form loss coefficient separately. In order to satisfy Eq. (43), the pipe length and the pipe diameter should be adjusted during the experimental facility construction, even the orifice should be added to the pipe system to make the resistance in the experiment resemble the prototype.

3.4.3. Thermal stratification in the containment scaling

Peterson et al. [21] reported the equation of the jet entering a large space, and defined the conditions for the stability of the large space stratification:

$$\left[\frac{(\rho_a - \rho_o) g d_o}{\rho_a u_o^2} \right]^{1/3} \frac{H_{Co}}{d_o} \left[1 + \frac{d_o}{4\sqrt{2}\alpha H_{Co}} \right]^{2/3} > 1 \tag{44}$$

The volume Froude number Fr_V is defined as Eq. (45),

$$Fr_V = \frac{\rho_a \dot{m}_{brk}^2}{\rho_o^2 g (\rho_a - \rho_o) H_{Co}^3 d_o^2 \left(\frac{\pi}{4}\right)^2} \tag{45}$$

Therefore, the conditions for the stability of the large space stratification can also be expressed as:

$$Fr_V < \left[1 + \frac{d_o}{4\sqrt{2}\alpha H_{Co}} \right]^2 \tag{46}$$

From Peterson's theory, the volume Froude number Fr_V is a characteristic parameter that evaluates the degree of break fluid mixing in a large space, so the volume Froude number Fr_V of the prototype and the experiment is equal, that is, $\{Fr_V\}_R = 1$, is the necessary condition to ensure that the thermal stratification state is similar in the prototype and the experimental containment in the accident.

The fluid properties of the break and the gas properties of the containment are all the same in the prototype and the experiment, so the similar conditions of thermal stratification in the containment can be further simplified as

$$\{Fr_V\}_R = \left\{ \frac{\dot{m}_{brk}^2}{H_{Co}^3 d_0^2} \right\}_R = \left\{ \frac{\dot{m}_{brk}^2}{H_{Co}^3 A_{brk}} \right\}_R = 1 \tag{47}$$

$$\{H_{Co}\}_R = \left\{ (A_{brk})^{-\frac{1}{3}} \right\}_R \left\{ \dot{m}_{brk}^{\frac{2}{3}} \right\}_R \tag{48}$$

When the break area scale ratio and the break mass flow rate are known, the break site axial position can be determined from Eq. (48).

3.4.4. Containment wall surface convection and condensation scaling

The heat transfer process near the containment wall surface is shown in Fig. 3, which mainly includes three heat transfer

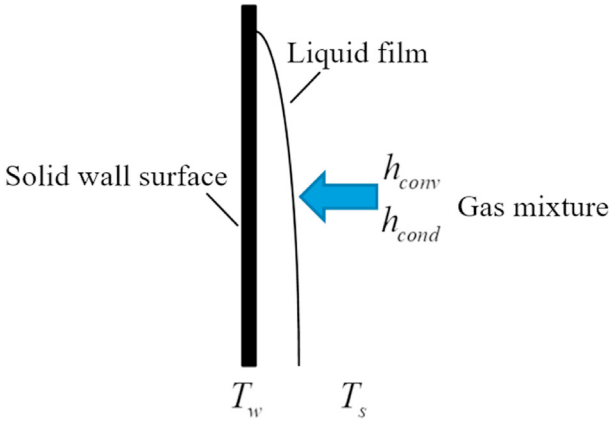

Fig. 3. Schematic diagram of film heat transfer.

mechanisms: condensate film heat conduction, mixed gas convection heat transfer and condensation heat transfer. Because the heat transfer coefficient of the liquid film heat conduction is far greater than the other two heat transfer coefficients, the heat transfer process of the liquid film heat conduction can be ignored. Under the postulated accident, the gas flow in the containment during the initial stage of the discharge is usually dominated by forced convection, while in the long-term stage of the discharge by the turbulent natural convection. In the containment analysis programs, such as WGOTHIC, all the gas convections on the wall surface are considered as turbulent natural convections for conservative considerations. Therefore, the same considerations are also preserved in this part.

In WGOTHIC, the McAdams relation [22] is used to calculate the convective heat transfer of the mixed gas:

$$h_{conv} = 0.13\frac{k}{L}\left(\frac{g\beta\Delta TL^3}{v^2}\mathrm{Pr}\right)^{1/3} \tag{49}$$

The condensation heat transfer is calculated by Kreith relation [23]:

$$\dot{m}''_{cond} = \frac{h_{conv}\rho_{stm}D_V}{k}\frac{\Delta p_{stm}}{p_{1m,a}}\left(\frac{Sc}{\mathrm{Pr}}\right)^{1/3} \tag{50}$$

$$h_{cond} = \frac{\dot{m}''_{cond}i_{fg}}{T_s - T_{sat}} \tag{51}$$

It can be seen from Eqs. (49) and (50) that h_{conv} and $\dot{m}''_{cond}$ are related to the physical property parameters, but not related to the geometric parameters. Because the same fluid (water vapor, air, and water) as the prototype is used in the test facility, the thermophysical properties of the gas/liquid in the experiment and the prototype are the same, so h_{conv} and $\dot{m}''_{cond}$ can be considered as the same.

3.4.5. Containment wall and in-containment component heat storage scaling

For the containment wall, the energy balance equation is as follow:

$$V_w\rho_w c_{p,w}\frac{dT_w}{dt} = h_c A_w(T_s - T_w) - h_{conv,o}A_w(T_w - T_a) \tag{52}$$

where the left-hand side represents the energy absorbed by the containment wall per unit time, the right-hand side represents the heat transfer power through the containment inside wall and outside wall respectively. As described in section 3.4.4, the heat transfer on the solid surface mainly composed of the condensation heat transfer and the convection heat transfer, then

$$(T_s - T_w) = q''(h_{cond} + h_{conv})^{-1} = q''h_t^{-1} \tag{53}$$

The equivalent heat transfer coefficient between the containment atmosphere and the containment inside wall is:

$$h_t = h_{cond} + h_{conv} \tag{54}$$

From Eqs. (49) and (51), h_t and $h_{conv,o}$ are only related to the physical properties, but not related to the geometrical parameters. Therefore, h_t and $h_{conv,o}$ are equal between the experiment and the prototype.

By normalizing Eq. (52) with appropriate reference values (i.e. $X^+ = X/X_{ref}$), the containment wall energy balance equation can be put in non-dimensional form as:

$$V_w^+\rho_w^+c_{p,w}^+\frac{dT_w}{dt} = \frac{h_{c,0}A_{w,0}(T_s - T_w)_0\tau_{cv}}{V_{w,0}\rho_{w,0}c_{p,w,0}T_{w,0}}h_c^+A_w^+(T_s - T_w)^+ - \frac{h_{conv,o,0}A_{w,0}(T_w - T_a)_0\tau_{cv}}{V_{w,0}\rho_{w,0}c_{p,w,0}T_{w,0}}h_{conv,o}^+A_w^+(T_w - T_a)^+ \tag{55}$$

To satisfy the similar containment wall heat storage condition in the prototype and the experiment, the following nondimensional similarity criterion can be obtained:

$$\left\{\frac{h_{c,0}A_{w,0}(T_s - T_w)_0\tau_{cv}}{V_{w,0}\rho_{w,0}c_{p,w,0}T_{w,0}}\right\}_R = 1 \tag{56}$$

$$\left\{\frac{h_{conv,o,0}A_{w,0}(T_w - T_a)_0\tau_{cv}}{V_{w,0}\rho_{w,0}c_{p,w,0}T_{w,0}}\right\}_R = 1 \tag{57}$$

Due to the same thermal physical properties in the prototype and the experiment, Eqs. (56) and (57) can be put into Eqs. (58) and (59), which is

$$\left\{\frac{A_{w,0}(T_s - T_w)_0}{V_{w,0}T_{w,0}}\right\}_R = 1 \tag{58}$$

$$\left\{\frac{A_{w,0}(T_w - T_a)_0}{V_{w,0}T_{w,0}}\right\}_R = 1 \tag{59}$$

It is important to note that Eq. (59) is used as a criterion only in long-term accident experiment, because the containment outside wall is assumed to be adiabatic in short-term transient.

As for the in-containment components, due to complex shape and various materials composition, it is hard to scale them accurately in the test facility. The current method is adding the same prototypical material with scaled mass in the test facility to simulate the heat absorption of this part. However, this method wastes both resource and time. Besides, the effectiveness is not guaranteed. Therefore, the energy absorption by this part will be considered from an integral effect in the experiment by means of decreasing the break down energy or adding the finned heat sink to increase the heat dissipation. After all the scaling parameters have been determined, the primary loop energy inventory and the blow down steam mass flow rate are adjusted by iteration to achieve the containment pressure response similitude.

3.4.6. Thermal stratification in the suppression pool scaling

For the thermal stratification caused by the vertical submerged steam jet, the characteristics of which is usually measured by Ri number [16]:

$$\mathrm{Ri}=\left(\frac{\rho_a-\rho_{jet}}{\rho_a}\right)\frac{gd_o}{u_o^2}\left(\frac{H_{Sp}}{d_o}\right)^2 \tag{60}$$

To resemble the thermal stratification/mixing phenomena in the experiment with the prototype, the Ri should be equal in both situations, that is, $\{\mathrm{Ri}\}_R = 1$.

Due to the same suppression pipe flow velocity and the material physical properties, Eq. (60) is simplified into Eq. (61).

$$\{H_{Sp}\}_R=\left\{\dot{m}_{in}\right\}_R\left\{d_o^{-3/2}\right\}_R \tag{61}$$

Thus, the suppression pipe exit position is determined.

3.4.7. Suppression pipe resistance scaling

The resistance characteristics of the suppression pipe can be expressed as the following equation:

$$\Delta p=\mathrm{p}_{Co}-p_{Sp}-\rho gH=\sum_i\left[\frac{f_i l_i}{d_i}+K_i\right]\frac{\dot{m}_i^2}{2\rho A_i^2} \tag{62}$$

$$\dot{m}_i=\frac{\dot{m}_{in}}{N} \tag{63}$$

If the pressure drop of the suppression pipe in the prototype and the test facility are equal, then the following equation should be met:

$$\{\Delta p\}_R=\left\{\sum_i\left[\frac{f_i l_i}{d_i}+K_i\right]\frac{\dot{m}_i^2}{2\rho A_i^2}\right\}_R=1 \tag{64}$$

That is,

$$\left\{\sum_i\left[\frac{f_i l_i}{d_i}+K_i\right]\right\}_R=\left\{\frac{A_i^2}{\dot{m}_i^2}\right\}_R=\frac{\left\{d_i^4\right\}_R\{N\}_R}{\{V\}_R} \tag{65}$$

In order to satisfy Eq. (65), the test facility pipe arrangement should be overall considered. The pipe length and the pipe diameter should be adjusted during the experimental facility construction, even the orifice should be added to the pipe system to make the resistance in the test facility resembles the prototype.

3.4.8. Vent clearing phase scaling

The vent clearing process can be expressed as follows [24]:

$$\Delta p=\rho_l l_{dpt}\frac{d^2 l_{dpt}}{dt^2} \tag{66}$$

Due to the same fluid used in the experiment and the similar pressure response both in the experiment and the prototype, by normalizing Eq. (66) with appropriate reference values, the equation can be put in non-dimensional form as:

$$\rho_l^+ l_{dpt}^+\frac{d^2 l_{dpt}^+}{dt^2}=\left\{\frac{\Delta p_0}{\rho_{l,0} l_{dpt,0}^2}\right\}\Delta p^+ \tag{67}$$

If the vent clearing process similarity is met, the following nondimensional similarity criterion should be satisfied,

$$\left\{\frac{\Delta p_0}{\rho_{l,0} l_{dpt,0}^2}\right\}_R=1 \tag{68}$$

Based on Eq. (68), the suppression pipe submerged depth can be determined.

4. Scaling criteria summaries

From the above top-down and bottom-up scaling analysis, a set of the scaling criteria are obtained and presented in Table .2.

Table 2
The scaling criteria.

Component phenomena	Scaling criteria	Scaling parameters
Containment pressure	$\left(\frac{V}{\dot{m}_{brk} i_{brk}}\right)_R = 1$	Mass and energy release; Containment free volume
Response	$\left\{\frac{\dot{m}_{cond}^{''} A_w}{V}\right\}_R = 1$	Effective heat transfer area of the containment wall
(top-down)	$\left\{\frac{h_{conv} A_w}{V}\right\}_R = 1$	
	$\left\{\frac{\dot{m}_{in}}{V}\right\}_R = 1$	Steam mass flow rate transported to the pressure suppression system
Pressure suppression	$\left\{\frac{V}{V_{pool,g}}\right\}_R = 1$	Pressure suppression system gas volume
system pressure response	$\left\{\frac{m_{stl}\Delta T_{stl}}{V}\right\}_R = 1$	Suppression pool component heat storage
(top-down)	$\left\{\frac{m_{pool,l}\Delta T_{pool,l}}{V}\right\}_R = 1$	Pressure suppression system water mass
Primary loop energy inventory	$\left\{\frac{V}{m_{loop} i_{loop}}\right\}_R = 1$	Primary loop water inventory
(top-down)	$\left\{\frac{\dot{m}_{ecc} i_{ecc}}{V}\right\}_R = 1$	Safety injection system water inventory
	$\left\{\frac{Q_{decay}}{V}\right\}_R = 1$	Core decay heat
Break blow down	$\left(\frac{V}{G_c A_{brk} i_{brk}}\right)_R = 1;$	Break area
(bottom-up)		

(*continued on next page*)

Table 2 (*continued*)

Component phenomena	Scaling criteria	Scaling parameters
	$\left(\frac{V}{G_{non-c}A_{brk}i_{brk}}\right)_R = 1$	
Primary loop resistance and the safety injection pipe resistance (bottom-up)	$\left\{\left(\frac{f_i l_i}{d_i}+\sum_i K_i\right)\frac{\dot{m}_i^2}{2\rho A_i^2}\right\}_R = 1$	Primary loop and safety injection loop geometrical parameters (pipe length/diameter, bend size/number, orifice size)
Thermal stratification in the containment (bottom-up)	$\{H_{Co}\}_R = \left\{(A_{brk})^{-\frac{1}{3}}\right\}_R \left\{\dot{m}_{brk}^{\frac{2}{3}}\right\}_R$	Break axial location
Containment wall surface convection and condensation (bottom-up)	$\{h_{conv}\}_R = 1$	Convective heat transfer coefficient
	$\{\dot{m}''_{cond}\}_R = 1$	Containment steam condensation rate
Containment wall and in-containment component heat storage (bottom-up)	$\left\{\frac{A_w(T_s-T_w)}{V_w T_w}\right\}_R = 1$	Containment wall and in-containment component volume
	$\left\{\frac{A_{w,0}(T_w-T_a)}{V_{w,0}T_{w,0}}\right\}_R = 1$	
Thermal stratification in the suppression pool (bottom-up)	$\{H_{Sp}\}_R = \{\dot{m}_{in}\}_R\{d_o^{-3/2}\}_R$	Suppression pipe exit location
Suppression pipe resistance (bottom-up)	$\left\{\sum_i\left[\frac{f_i l_i}{d_i}+K_i\right]\right\}_R = \frac{\{d_i^4\}_R\{N\}_R}{\{V\}_R}$	Suppression loop geometrical parameters (pipe length/diameter, bend size/number, orifice size)
Vent clearing (bottom-up)	$\left\{\frac{\Delta p}{\rho_l l_{dpt}^2}\right\}_R = 1$	Suppression pipe submerged depth

5. Conclusions

A scaling method that follows the H2TS principles was proposed, by which the scaling analysis was conducted on a conceptual small PWR LOCA transient, aiming to reproduce the important thermal hydraulic phenomena both in the containment and the pressure suppression system. The main remarks are concluded below:

(1) The dominant phenomena that occurred in the system are identified at first. Under the reasonable assumptions, the pressure response of the containment and the pressure suppression system was analyzed through the top-down scaling method, while the important local phenomena were analyzed through the bottom-up scaling method. A set of the scaling criteria were obtained, through which the main parameters of the test facility can be determined.
(2) Since the pressure response in the containment and the steam condensation in the suppression pool are influenced by many different factors, it turns out to be impossible or impractical to achieve exact dynamic similarity between a small-scale system and a full-scale one. The scaling criteria put forward should be considered overall when applied. The most important phenomena should be preserved as a first consideration. Then the maximum similarity between the prototype and the experiment can be achieved.
(3) Following the scaling criteria proposed in this paper, a scaled down test facility can be designed and the relevant experimental research on the passive containment pressure suppression system characteristics under the accident scenarios can be conducted.
(4) The assessment of scaling distortion needs to be accomplished in the future to improve the research work.

Declaration of competing interest

The authors declare that they have no known competing financial interests or personal relationships that could have appeared to influence the work reported in this paper.

Acknowledgements

The financial supports of Heilongjiang Province Postdoctoral Fund (002150830605) and Fundamental Research Funds for Central University of Ministry of Education of China (3072019CF1506) are gratefully acknowledged.

Nomenclature

A	area, m^2
a	velocity acceleration, m/s^2
c_p	specific capacity, J/kg
d	diameter, m
D_v	gas diffusion coefficient, dimensionless
f	resistance coefficient, dimensionless
G	break mass flux, $kg/(m^2\cdot s)$
h	heat transfer coefficient, $J/(m^2\cdot{}^\circ C)$
H_{Co}	length from the break to the containment top, m
H_{Sp}	length from the pipe exit to the suppression pool bottom, m
i	enthalpy, J/kg
k	thermal conductivity, $W/(m\cdot K)$
K	form loss coefficient, dimensionless
L	length, m
L	characteristic length, m
m	mass, kg
$\dot{m}$	mass flow rate, kg/s
$\dot{m}''$	mass flux, $kg/(m^2\cdot s)$
N	pipe number, dimensionless
p	pressure, Pa
q''	heat flux, W/m^2
Q	decay power, W
s	specific entropy, $J/(kg\cdot K)$
t	time, s
T	temperature, °C
u	velocity, m/s

V	volume, m^3
x	dryness, dimensionless

Greek letters

α	Taylor's jet entrainment constant
β	gas expansion coefficient, dimensionless
γ	ratio of specific heats, dimensionless
τ	system response time, s
ρ	density, kg/m^3
ν	specific volume, m^3/kg
υ	kinematic viscosity, m^2/s
δ	pipe outlet thickness, m
Π_p	universal scale parameters
Δ	difference

Subscripts

a	ambient
brk	break
c	critical
Co	containment
cond	condensation
conv	convection
conv,o	outside wall convection
cv	control volume
decay	decay heat
dpt	submerged depth
ecc	safety injection
exp	expansion
f	fluid
fg	phase-change parameters
g	gas
i	sequence number
in	flow into the pressure suppression system
jet	gas jet
l	liquid
lm	logarithmic differential
loop	reactor primary loop
non-c	noncritical
o	outlet
pool	suppression pool
Pr	primary loop
R	ratio of the test facility to the prototype
s	steam
sat	saturation
Sp	suppression pool
srf	surface
srk	shrink
stl	steel
stm	steam
t	total
w	containment wall
0	reference value

Superscripts

+	nondimensional variables

References

[1] Biao Quan, et al., Research on suppressant characteristics of suppression containment, Nucl. Power Eng. 35 (2) (2014) 114–117.
[2] Studsvik, A.B. Energiteknik, Marviken Full-Scale Critical-Flow Tests. Volume 22. Results from Test 14. Final Report. No. EPRI-NP–2370-VOL. 22, Studsvik Energiteknik AB, 1982.
[3] H.G. Thoren, et al., Full-scale Containment Experiments Performed in the Marviken Power Plant. No. CONF-730304–, 1973.
[4] Yutaka Kukita, et al., The noncondensable gas effects on loss-of-coolant accident steam condensation loads in boiling water reactor pressure suppression pool, Nucl. Technol. 63 (2) (1983) 337–346.
[5] Jani Laine, Markku Puustinen, Antti Räsänen, PPOOLEX Experiments on the Dynamics of Free Water Surface in the Blowdown Pipe. No. NKS–281, Nordisk Kernesikkerhedsforskning, 2013.
[6] G. Patel, V. Tanskanen, R. Kyrki-Rajamäki, Numerical modelling of low-Reynolds number direct contact condensation in a suppression pool test facility, Ann. Nucl. Energy 71 (2014) 376–387.
[7] G. Patel, et al., Direct contact condensation modeling in pressure suppression pool system, Nucl. Eng. Des. 321 (2017) 328–342.
[8] Amir N. Nahavandi, Frank S. Castellana, Edick N. Moradkhanian, Scaling laws for modeling nuclear reactor systems, Nucl. Sci. Eng. 72 (1) (1979) 75–83.
[9] G. Kocamustafaogullari, M. Ishii, Scaling of two-phase flow transients using reduced pressure system and simulant fluid, Nucl. Eng. Des. 104 (2) (1987) 121–132.
[10] Novak Zuber, et al., An integrated structure and scaling methodology for severe accident technical issue resolution: development of methodology, Nucl. Eng. Des. 186 (1–2) (1998) 1–21.
[11] W.L. Brown, Scaling of the AP600 containment large scale test facility, in: 7th International Conference on Nuclear Engineering, Japan Society of Mechanical Engineers, Tokyo, Japan, 1999.
[12] Jose N. Reyes Jr., Hochreiter Lawrence, Scaling analysis for the OSU AP600 test facility (APEX), Nucl. Eng. Des. 186 (1–2) (1998) 53–109.
[13] Pravin Sawant, Mohsen Khatib-Rahbar, Modeling pressure suppression pool hydrodynamics in the ABWR containment, Nucl. Eng. Des. 241 (9) (2011) 3824–3838.
[14] Tangtao Feng, et al., Numerical research on thermal mixing characteristics in a 45-degree T-junction for two-phase stratified flow during the emergency core cooling safety injection, Prog. Nucl. Energy 114 (2019) 91–104.
[15] Mingjun Wang, et al., Study on the coolant mixing phenomenon in a 45° T junction based on the thermal-mechanical coupling method, Appl. Therm. Eng. 144 (2018) 600–613.
[16] Robert E. Gamble, et al., Pressure suppression pool mixing in passive advanced BWR plants, Nucl. Eng. Des. 204 (1–3) (2001) 321–336.
[17] Shinya Mizokami, et al., Unsolved issues related to thermal-hydraulics in the suppression chamber during Fukushima Daiichi accident progressions, J. Nucl. Sci. Technol. 53 (5) (2016) 630–638.
[18] L.I. Sheng-Qiang, L.I. Wei-Hua, J. Sheng-Yao, Study on source term evaluation method in simulation and scaling for containment during LOCA, Nucl. Power Eng. 33 (3) (2012) 132–137.
[19] Frederick J. Moody, Introduction to Unsteady Thermofluid Mechanics, Wiley-Interscience, New York, 1990, p. 667, 1990.
[20] Robert E. Henry, Hans K. Fauske, The two-phase critical flow of one-component mixtures in nozzles, orifices, and short tubes, 1971, pp. 179–187.
[21] P.F. Peterson, V.E. Schrock, R. Greif, Scaling for integral simulation of mixing in large, stratified volumes, Nucl. Eng. Des. 186 (1–2) (1998) 213–224.
[22] W.M. Rohsenow, H. Choi, Heat, Mass, and Momentum Transfer, 1961.
[23] Frank Kreith, Raj M. Manglik, Mark S. Bohn, Principles of Heat Transfer, Cengage learning, 2012.
[24] Richard T. Lahey, F.J. Moody, The Thermal-Hydraulics of a Boiling Water Nuclear Reactor, second ed., 1996.